Modeling and Simulations of Solar Bidirectional Substation

Lamaison Nicolas, David Chèze, Cedric Paulus, Roland Baviere

MODELING AND SIMULATIONS OF SOLAR TWO-WAY SUBSTATION

Nicolas Lamaison[1,2], David Chèze[1,2] and Cédric Paulus[1,2]
CEA LITEN - 17 Rue des Martyrs, 38054 Grenoble (France)
INES - 50 Avenue du Lac Léman, 73375 Le Bourget du Lac (France)
+33 479792153, nicolas.lamaison@cea.fr

Abstract – Decentralized surplus feed-in of solar heat into a District Heating Network (DHN) is here addressed. The heat collected from solar panels located on rooftops of DHN connected buildings may either be used locally for domestic hot water and space heating or fed into the DHN. Two-way substations able to transfer heat from and into the network seem then to be required utilities. The present paper presents the specifications (60kW capacity, return-to-supply connection) and promising architectures of such two-way substation based on a previous analysis. A first-of-a-kind Modelica-based dynamic model of the substation together with the consumer and the solar field connected to it is then detailed. Two-day simulations considering real operating conditions of DHN were then performed. The results highlighted i) the good match between the periods of solar heat reinjection with the periods of low supply temperature and differential pressure and ii) the decisive benefit of the reinjection to increase the part of useful solar energy.

1. INTRODUCTION

In the "2way District Heating" course of action from the 4GDH concept (Lund et al., 2014), decentralized feed-in of solar heat from prosumers seems to be a promising solution to increase the share of renewable energy in District Heating Networks (DHN), especially in dense urban areas with limited ground surface. However, when scattered customers roofs are used to collect and inject heat locally in a network, new problematics arise. Local consumption or total feed-in of the collected solar energy, use of storage at the building level, and management of the local differential pressure and supply temperature are the most decisive ones.

Among the various reinjection principles, Return to Supply feed-in is considered since it seems to be the most flexible option from the DHN point of view (Beckenbauer et al., 2017; Lennermo and Lauenburg, 2016; Schäfer and Schmidt, 2016). However, R/S feed-in implies to overcome the local differential pressure between the return and supply lines, which usually exhibits significant variations due to rapid load fluctuations. Moreover, the feed-in temperature must be superior or equal to the local network supply line temperature. The latter constraints on the local differential pressure and the local supply temperature involve at the two-way substation level the use of at least a variable speed pump and a finely tuned control strategy.

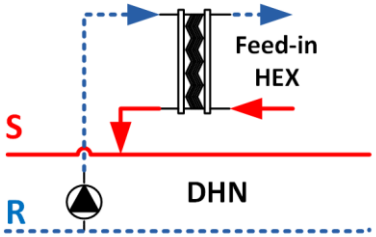

Figure 1: Schematic of Return to Supply (R/S) feed-in

At the network scale, various studies investigate decentralized reinjection and its effect on the thermo-hydraulic behavior of the network (Brange et al., 2016; Hassine and Eicker, 2014; Heymann et al., 2017). However, at the component scale i.e. the substation, only few studies from the open literature address the topic of the reinjection. From the simulation point of view, Paulus and Papillon (2014) compared nine different substation architectures, however connected in a Return to Return fashion, using TRNSYS and evaluated the influence of the return temperature, solar collectors area and type of solar collectors on thermal performances only. From the experimental point of view, Rosemann et al. (2017) addressed the challenging topic of innovative control algorithm at the substation level with Hardware-In-The-Loop testing. There conclusions were used to build various first-of-a-kind solar prosumers and decentralized feed-in substations (Rosemann et al., 2017a).

In the frame of the Horizon 2020 "THERMOSS" project, specifications, modelling and prototype testing of a two-way substation for a multi-family building is performed.

In the present paper, specifications and promising architectures are first presented in the basis of what was presented in Lamaison et al. (2017). Second, a first-of-a-king Modelica-based dynamic model of the most promising two-way substation together with the consumer and the solar field connected to it is then detailed. The control strategies and operating principles associated to this substation are then discussed. Third, results of a two-day simulation considering real DHN operating conditions in terms of differential pressure and temperatures (supply and return) is then detailed in terms of temperatures, flow rates and heat power. Finally, a sensitivity analysis on the DHN operating conditions is presented.

2. SPECIFICATIONS AND ARCHITECTURE

2.1 Specifications

During the first year of the THERMOSS project, specifications and architecture of a two-way substation were addressed. In order to give a precise frame to study, it was decided to specifically consider the decentralized reinjection of solar heat on a DHN. Extrapolation to other local heat sources is also envisioned and will use the current development as basis.

As stated in the Introduction, R/S feed-in is considered since it is the most promising option. As highlighted schematically in Figure 2, the solar collectors are assumed to be on the rooftop of a multi-family building, equipped with a unique two-way substation. Variants relying on individual two-way stations at the apartment level have been discarded from this study due to prohibitive cost and increased complexity. Indeed, solar two-way substations seem more appropriate for multi-family buildings rather than for individual apartments (Rosemann et al., 2017b) since it simplifies the hydraulic connections at the building level while reducing the costs. It also reduces the number of reinjection points in the DHN, aggregate heat inputs and thus simplifies the operation of the network.

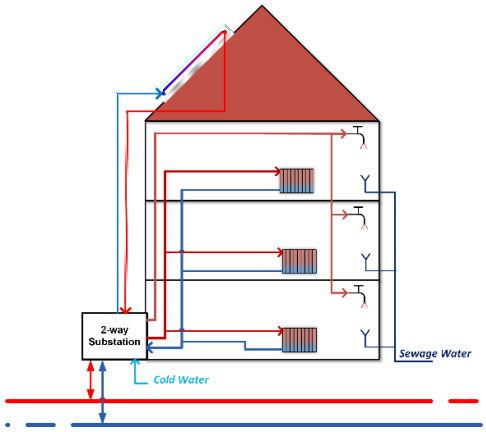

Figure 2: Schematic of a two-way substation in a multi-family building prosumer

Regarding the order of magnitudes involved for the present study, it is considered that the building consists in 6 apartments of 70m² organized in 3 floors of 2 apartments, leading to a building footprint of 7.5m of height, 10m of width and 14m of length. Firstly, assuming a rather poorly insulated envelope, the required Space Heating (SH) power is approximately 42kW (i.e. around 100W/m²). Secondly, using the daily draw-offs from COSTIC (2016), i.e. about 150 liters for an apartment of 3 people, and the "DHW-calc" calculator (Jordan and Vajen, 2005) to obtain a distributed daily profile, the maximum 10 minutes average is about 16kW/apartment. The latter leads to 60kW of Domestic Hot Water (DHW) power consumption for the entire building when accounting for a simultaneity coefficient of 0.62. Finally, accounting for the building geometry, it is calculated that the maximum solar collector area is about 80m² (which covers one side of the rooftop with a 30° of inclination angle). The building solar production would reach 56kW with an assumption of 700W/m² of production based on IEA SHC recommendations (IEA SHC, 2004).

2.2 Substation architectures chosen

The present work is a continuation of the study presented in (Lamaison et al., 2017) that discussed the possible architectures of such two-way substation based on a set of features and selected the most promising ones based on a set of criteria.

Features such as the location of the hydraulic separation between the network and the building, local consumption of the heat or total feed-in and control strategies were combined to build an exhaustive list of possible configurations. Promising setups were chosen from that list based on a multi-criteria analysis (cost, operation, ownership, etc.). These setups are presented in Figure 3, Figure 4 and Figure 5. The two first architectures exhibit complete reinjection of the solar heat on the network without direct local consumption of this heat while the last one promotes a local usage for DHW preheating while reinjecting the excess heat into the network.

On the three Figures, various control strategies are highlighted (S0, S1 and S2). The goal of these control strategies is to obtain a feed-in temperature level above the local supply temperature in the DHN, while also addressing the following constraints:

i) Minimize the temperature in the solar field to reach high efficiencies,
ii) Overcome the strongly varying local flow resistance, i.e. differential pressure drop,
iii) Adjust the feed-in flow rate so that the feed-in rate matches the strongly varying heat rate produced by the solar field.

S0 consists in a pump and a valve in series, S1 consists in a pump and a bypass valve, and S2 consists in a hydraulic separator and two pumps. It should be noted that for the present study, only Architecture 2 (C2U0) with control strategy S0 is considered.

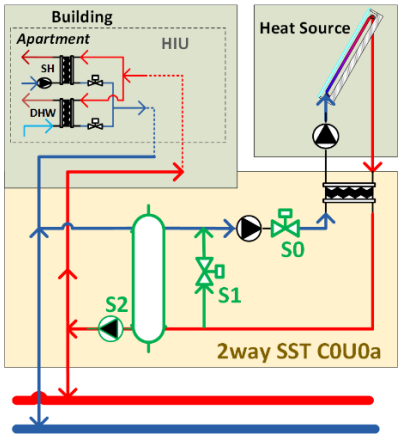

Figure 3: Schematic of Architecture 1 (C0U0)

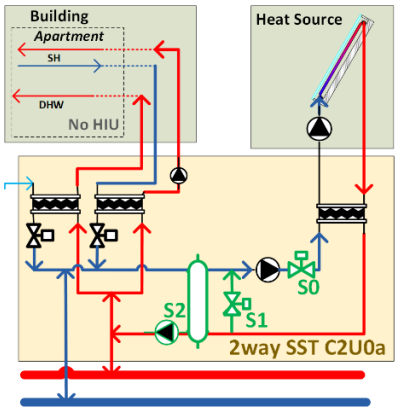

Figure 4: Schematic of Architecture 2 (C2U0)

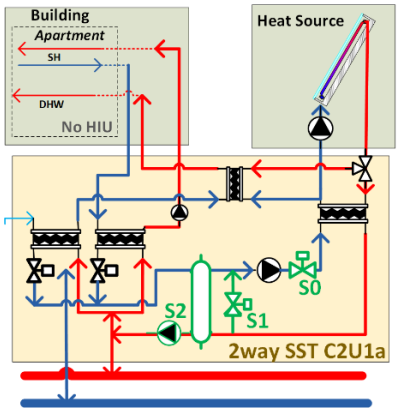

Figure 5: Schematic of Architecture 3 (C2U1)

3. MODELING

The present section introduces first the modelling framework. Second, it presents in sequence the models for the consumer (SH and DHW), the solar field and the substation. Third, the network boundary conditions used in the present study are highlighted. Finally, the control associated to the operation of the substation and the basic operating principles are discussed.

3.1 Modelling Framework

The modelling framework is based on the open source modelling language Modelica used in the commercial simulation environment Dymola. Modelica is an acausal (equation-base) and object-oriented programming language with a large and fast-growing community both for industrial and academic applications (Schweiger et al., 2017). Modelica has native multi-physical modelling capabilities (thermo-hydraulic), is structured in libraries enabling exchange of methods in the scientific community and allows for implementing new components. Moreover, the Annex 60 project from the IEA (Wetter, et al., 2015) promotes the development of computational tools for building and community energy systems based on Modelica and FMI standards, motivating the choice of this modelling framework.

As mentioned in the introduction, the Modelica "Standard" Library for its common connectors and fluid ports, the "Buildings" library (Wetter et al., 2014) for its general building models and the "DistrictHeating" library (Giraud et al., 2015) for its DHN piping and solar collectors models will be used.

3.2 Consumer

The consumer is modelled in terms of space heating consumption using the 'Buildings' library (Wetter et al., 2014) from Modelica and in terms of domestic hot water consumption using the 'DHW-calc' draw-offs profile (Jordan and Vajen, 2005).

Space heating is modelled with i) a heating system and ii) a mono-zone building. Concerning the heating system, it is composed of a thermostatic valve and a radiator modelled using the "RadiatorEN442_2" model from the library "Buildings" (Wetter et al., 2014). In this model, the transferred heat is computed using a discretization along the water flow path, and heat is exchanged between each compartment and a uniform room air and radiation temperature. Concerning the mono-zone building, it is modelled using the "mixed air" model (Wetter et al., 2011) from the same library. It considers a perfectly mixed air in the room and takes into account heat exchange through convection, conduction, infrared radiation and solar radiation. Internal heat gains due to occupation (latent heat), lighting (radiation) and home appliances (convection) are included in the model. Constant single-flow ventilation is considered with a flow-rate of about 0.4 room volume per hour. For the present study, the dimension of the building considered were listed in Section 2.1. The total glazed area for the building represents 1/6 of the building living area, shared as follows, 50% on the South wall, 15% on the West wall and 35% on the East wall. The envelope of the building (layers composition and infiltration) is set to follow the RT2000 French thermal regulations.

Concerning the equivalent radiator, it is assumed to have a nominal inlet temperature, a nominal difference and a nominal power of respectively 70°C, 15K and 42kW. For the obtained nominal mass flow rate of 0.7kg/s, a nominal pressure drop of 1bar is assumed (together with a quadratic pressure drop law). The set point for the building ambient temperature is set at 20°C.

The model requires as inputs the outside temperature and the set point for the radiator inlet temperature. In the present study, the analysis of the operation of the two-way substation is studied for 2 days. Thus, Figure 6 gives this 2 days outside temperature profile calculated using the weather station of Chambéry-Aix les Bains in the software Meteonorm (2017). The 2 days considered are the 11 and 12th of March. The associated set point for the thermostatic valve is also given in Figure 6. The latter follows a heating curve, i.e. 60°C as radiator inlet set point temperature for -10°C as outside temperature and 25°C for 15°C).

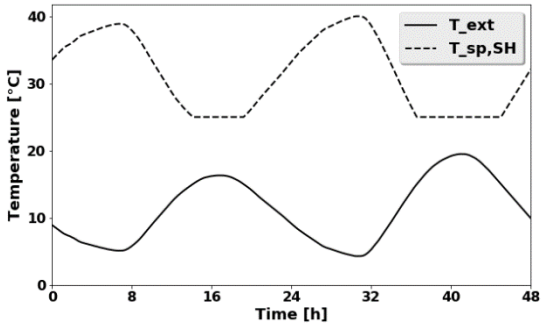

Figure 6: Two days outside temperature and associated radiator inlet temperature set point profiles

The water draw-off system is considered without sanitary loop. As explained initially, the daily profile of draw-offs are obtained from the software DHW-calc (Jordan and Vajen, 2005) from Task 26 of IEA which distributes DHW draw-offs throughout the year or the day with statistical means, according to a probability function. The mean daily DHW consumption was set to 900litres, i.e. 150l/apartment. The latter was obtained from a report of COSTIC (2016) based on the type of apartment and the number of people living in it. Figure 7 shows the 2 days profile considered (6 minutes time-step). The cold water temperature is considered constant equal to 10°C.

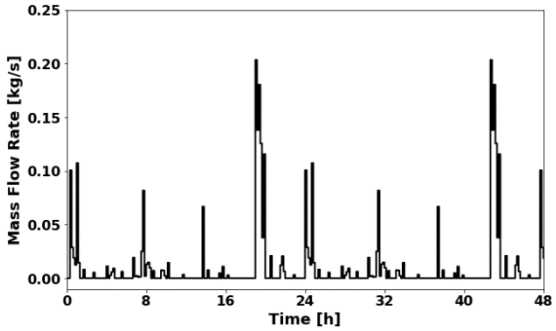

Figure 7: Two days DHW draw-offs profile at 10 minutes time step (obtained from DHW-calc software)

3.3 Solar Field

The solar field on the rooftop is modelled using a component developed inside the 'DistrictHeating' library specifically for the present study. It is a thermo-hydraulic model that considers collectors arranged in rows, each row being discretized in a number of element superior or equal to the number of collectors in the row. The energy balance of each discretized element follows is shown in Eq.(1) which comes from the norm NF EN ISO 9806 (2017).

In that equation, the thermal capacity C accounts for the fluid and material capacities, T_m is the mean temperature of the fluid through the field, T_a is the ambient temperature, A_{field} refers to the total collector field area, η_0 is the collector optical efficiency and a_1 and a_2 are respectively the linear and quadratic heat loss coefficients. The three latter coefficients are obtained using the Solar Keymark test results report ("Solar Keymark Database," 2018).

Finally, in Eq.(1), G_T is calculated using Eq.(2) in which I_b and I_d are the direct and diffuse solar irradiations, obtained from weather data and K_b and K_d are the incidence angle modifiers for the direct and diffuse irradiations, obtained from the Solar Keymark test results report ("Solar Keymark Database," 2018). More specifically, K_b depends on the incidence angle θ and is obtained using input table from manufacturer.

$$C\frac{dT_m}{dt} = A_{field}(\eta_0 G_T - a_1(T_m - T_a) - a_2(T_m - T_a)^2) + \dot{m}_{sol}cp(T_{in} - T_{out}) \quad (1)$$

$$G_T = I_b K_b + I_d K_d \quad (2)$$

The direct irradiation I_b and incidence angle θ must be calculated on the tilted plan of the collectors while to obtain the diffuse irradiation I_d on the tilted surface, the model of Perez et al. (1990) is used. For both irradiation calculations, the horizontal solar irradiation obtained from the weather station of Chambéry-Aix les Bains in the software Meteonorm (2017) is used. Figure 8 presents the resulting total solar irradiation for the 2 days considered.

Hydro-dynamically speaking, the mass flow is considered perfectly distributed in the different rows for the present study. Thus, the solar field pressure drop is calculated with a quadratic law using the total solar loop flow rate $\dot{m}_{sol}$, the single collector nominal pressure drop $\Delta P_{nom,c}$ and flow rate $\dot{m}_{nom,c}$, and the number of rows N_{rows} and collectors per row $N_{coll\_per\_row}$, as shown by Eq. (3).

$$\Delta P_{solar,field} = N_{coll\_per\_row}\Delta P_{nom,c}\left(\frac{\dot{m}_{sol}}{N_{rows}\dot{m}_{nom,c}}\right)^2 \quad (3)$$

Finally, there are two pipes on the solar field (return and supply lines) modelled using finite volumes with heat losses (see Eq. (4) with 'z' being the abscissa along the pipe and UA_{loss} the overall heat transfer coefficient). For the heat losses, the piping are considered to be in contact with the ambient air. The pressure drop in this piping also follows a quadratic law (see Eq. (5)).

$$C\frac{dT}{dt} = \dot{m}cp\frac{dT}{dz} - UA_{loss}(T - T_{ext}) \quad (4)$$

$$\Delta P_{pipe} = \Delta P_{nom,pipe}\left(\frac{\dot{m}}{\dot{m}_{nom,pipe}}\right)^2 \quad (5)$$

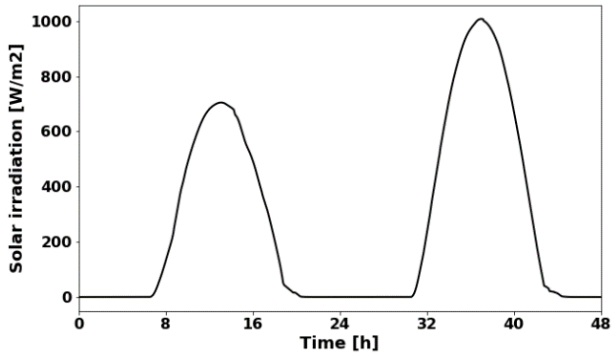

Figure 8: Total (diffuse + direct) solar irradiation on the tilted plan (30°) of the solar collectors for 2 days considered

In the present study, two rows of two double-glazing solar thermal panels ("SavoSolar SF500-15DG - Solar Keymark," 2016) with a gross unit area of 15.96m² (2.6m x 6.2m) leads to a gross area of about 64m² (5.2m x 12.4m) that fits in the estimated space in Section 2.1. The solar collector coefficients and unit capacity are respectively 0.793, 2.52 W/m²/K, 0.004W/m²/K and 12 KJ/K/m². Both the supply and return lines of the solar field are considered to be 20m long with an internal diameter of 32mm and insulated with 3cm of PUR Foam.

3.4 Substation

As shown in Figure 9, the C2U0 two-way substation is modelled with 3 Heat Exchangers, 2 valves and 2 pumps. Concerning the heat exchangers (HEX_{sol}, HEX_{DHW} and HEX_{SH}), they are discretized with finite volume method on both sides. A constant overall heat transfer UA is assumed, sized for the nominal operating conditions listed in Table 1 below.

Table 1: Heat Exchanger sizing

HEX	Thot,in [°C]	Thot,out [°C]	Tcold,in [°C]	Tcold,out [°C]	Q [kW]
Solar	90	60	50	80	60
DHW	80	45	10	45	60
SH	80	50	40	70	42

The service lines between the network and the substation are modelled using the finite volume model of long pipes form the 'DistrictHeating' library (Giraud et al., 2015). The flow in these lines can switch direction. They are sized for 60kW for a temperature difference of 30°C. The latter means a flow rate of 0.47kg/s, which leads to a DN32 for a nominal pressure drop of 100Pa/m (usual sizing value for DHN). The nominal velocity is thus calculated to be about 0.6m/s below the advised limit of 2m/s. A quadratic model (similar to Eq. (5)) is then used to obtain the pressure drop during the simulations. A length of 50m is chosen for these service lines with an insulation of 3cm of PUR Foam.

For the consumer two-way valves (V_{SH} and V_{DHW}), a linear characteristic is considered assuming that the nominal flow rate of 0.47kg/s should be ensured for a differential pressure drop of 1bar. For the SH pump (P_{SH}), it is assumed to operate at a constant differential pressure drop of 1bar in accordance with the equivalent radiator characteristics as described in Section3.2.

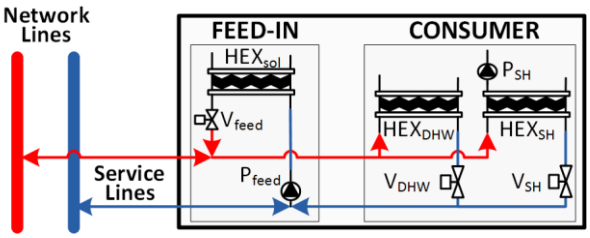

Figure 9: Two-Way Substation model (Similar to Figure 4 with S0 strategy only)

Finally, the feed-in pump (P_{feed}) is considered to be subjected to the network pressure drop and its flow rate is controlled as explained later in Section 3.6. For the calculation of the feed-in pump consumption, an isentropic efficiency of 80% is accounted for.

3.5 Network boundary conditions

The network side inputs are the local differential pressure and supply/return temperatures. In the present model, these two variables can either be set to constants to study specific operational conditions or set to follow real DHN variations. For the latter, data were collected by Veolia Giroa in the frame of the THERMOSS project at the DHN of San Sebastian, Spain. Figure 10 below presents these data for the two consecutive days of interest (2nd and 3rd of March 2017) with a time step of 15 minutes. These data are here only used as typical DHN data and are not correlated to the other boundary conditions such as the outside temperature for example.

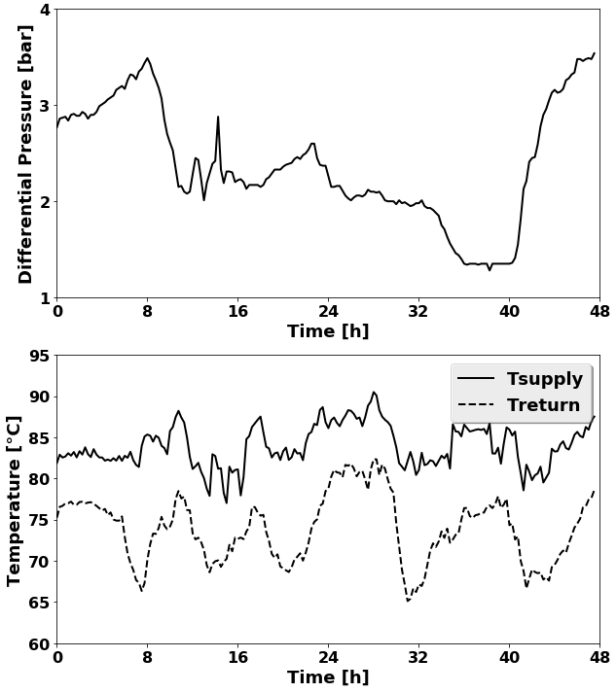

Figure 10: Differential Pressure and Supply/Return Temperatures used as DHN inputs for the simulations

3.6 Control and Operating Principles

The control strategy of the two-way substation concerns first the valves on the consumer side, second the solar field pump speed and third, the feed-in pump speed:

- Consumers: The DHW valve (V_{DHW}) opening is controlled using a pure proportional controller so that the secondary hot temperature on the consumer side is equal to 45°C. Similarly, a pure proportional controller is used for the opening of the SH valve (V_{SH}) so that the secondary hot temperature is equal to the set point defined in Figure 6.
- Solar field: The solar field pump starts when the irradiation in the plane of the solar field is above 100W/m² and its flow rate is controlled by a PI controller so that the outlet temperature of the solar field is constant (set at the DHN supply temperature plus a margin of 10°C). The flow rate on the field is bounded between 10 and 50 kg/hr/m² of solar panels.
- Feed-In: The feed in pump (P_{feed}) starts when the solar field outlet temperature is above the supply temperature of the DHN plus a margin of 5°C. The speed of the feed-in pump is controlled so that the outlet temperature of the feed-in heat exchanger is above the supply temperature of the DHN plus a margin of 5°C.

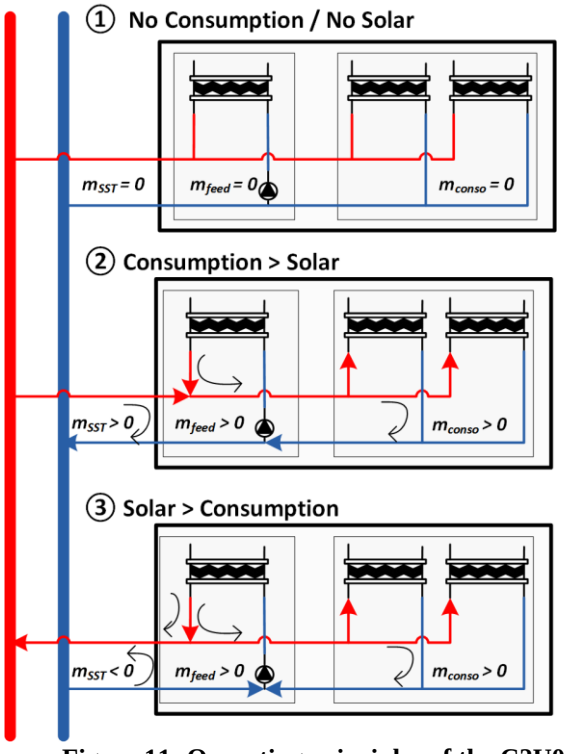

Figure 11: Operating principles of the C2U0 Substation

The operating principles of the substation are presented in Figure 11. At a given instant of time, there are three cases possible:

i) In case 1, there is no heat consumption or solar production and thus there is no flow through the service lines;
ii) In case 2, the heat consumption for domestic hot water and space heating is larger than the solar production. The solar energy is used for the consumer needs in addition to the heat coming from the network. The flow in the service lines is thus from the supply to the return line;
iii) In case 3, the heat consumption is lower than the solar production. The solar energy is used to entirely satisfy the consumer needs and the surplus heat is reinjected to the network. The flow in the service lines is thus from the return to the supply line.

4. SIMULATION RESULTS

4.1 Two days operation analysis

Figure 12 presents first the results in terms of mass flow rate in the solar field, from the network, from the feed-in pump and to the consumer (DHW+SH). The 3 operating cases described in the previous Section are specifically highlighted. The peaks in the consumer flow rates are due to the DHW draw-offs. The oscillations observed for the feed-in are due to the PI controller that requires a better identification, or even a gain schedule-like identification due to the strongly varying operating conditions. The conclusion of this graph is that reinjecting the solar heat on the network when no local storage facilities are available is of prime interest since the solar production periods do not match the local consumption periods.

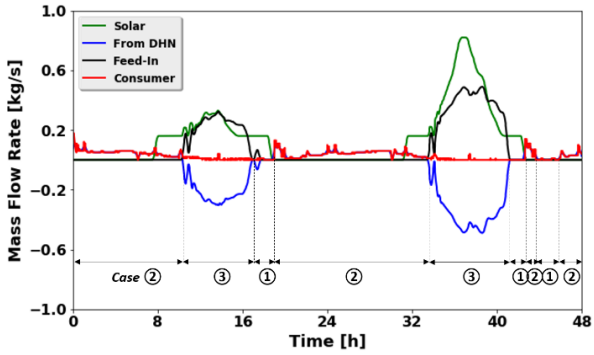

Figure 12: Mass flow rates in the two-way substation and in the solar field for the 2-days simulation period

Figure 13 presents the results of the 2days simulation in terms of temperature. The periods of consumption and reinjection are noticeable on the temperature chart, i.e. when the temperature at the entrance of the service line is the same as the DHN supply temperature, the substation consumes heat, when it is above, it reinjects heat. It is here interesting to note that solar energy production periods are coincident with the periods where the heating demand is the lowest (due to high outside temperature and passive gains) for which in general the supply temperature from the network is also the lowest. The latter is favourable for

the reinjection. A similar analysis can be performed for the network differential pressure.

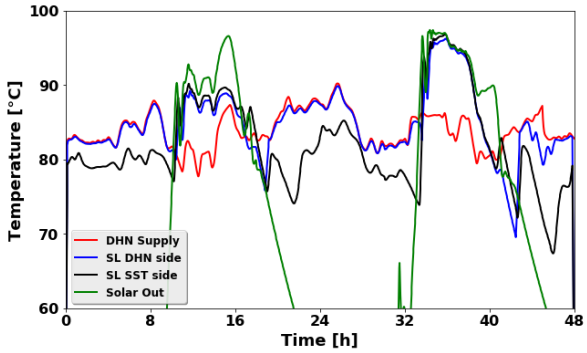

Figure 13: Temperatures in the supply line of the DHN, the supply service line (SL) and the solar field for the 2-days simulation period

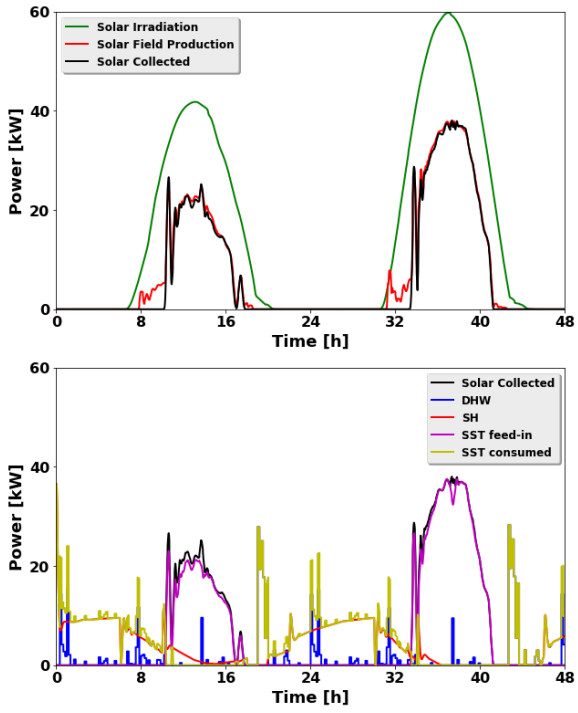

Figure 14: Heat power in the substation for the 2-days simulation period

Figure 14 presents the results of the 2days simulation in terms of heat power. On the top chart, the difference between the solar irradiation (Q_{sol}) and the solar field production (Q_{field}) is due to the solar collectors' efficiency. The difference between the solar field production (Q_{field}) and the collected energy (Q_{coll}) is due to the losses in the solar field piping mostly during the start-up phase (warming up of the volume of water that cooled down at night). On the bottom chart, all the heat power related to streams from or to the two-way substation are shown. It is worth noticing that the part of self-consumption is rather small (SH and DHW curves below the Solar Collected curve). A schematic explanation of all the heat power from Figure 14 is given in Figure 15.

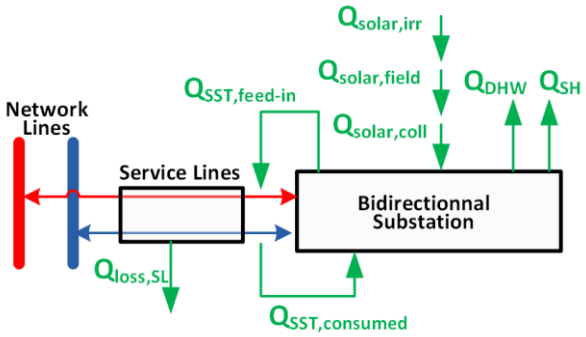

Figure 15: Schematic of the power streams used in Figure 14

4.2 Influence of DHN differential pressure, supply temperature and return temperature

Using the previous simulation as a base case scenario, 3 additional simulations for which respectively the DHN differential pressure was increased by 1bar, the DHN supply temperature was increased by 10°C and the DHN return temperature was reduced by 10°C were performed. Table 2 summarizes the results in terms of energy, using the same nomenclature as Figure 15. The feed-in pump consumption is also calculated. In general, the increase of the differential pressure has only an impact on the feed-in pump consumption while an increase of either the supply or the return temperature will reduce the solar plant production (lower field efficiency and larger heat losses).

Table 3 presents 5 ratios of interest using the energies presented in Table 2. As shown before, both the efficiencies of the solar field ($E_{solar,field}/E_{solar,irr}$) and the plant ($E_{solar,coll}/E_{solar,irr}$) are reduced with an increase of either DHN lines temperature. Additionally, the ratio of the self-consumed solar energy ($E_{solar,coll}$- $E_{loss,SL}$) to the total energy consumed (E_{SH}+E_{DHW}) referred as $\eta_{self\_vs\_cons}$ and to the collected solar energy referred as $\eta_{self\_vs\_solar}$ are rather small when considering that the solar energy produced is larger than the consumed energy. The reinjection is thus primordial in such situation since it transforms the collected solar energy into useful energy (for other DHN users). Finally, the pump ($E_{feed,pump}$) to collected solar energy ($E_{solar,coll}$) referred as $\eta_{pump\_vs\_solar}$ increases with a higher differential pressure and decreases with higher supply and lower return temperature.

Table 2: Sensitivity on DHN operating conditions (unit: kWh)

Case	Base	ΔP+1bar	T_s+10°C	T_r-10°C
$E_{solar,irr}$	760.19	760.19	760.19	760.19
$E_{solar,field}$	361.13	361.09	342.63	372.78
$E_{solar,coll}$	332.74	332.71	310.58	345.04
E_{SH}	194.28	194.42	194.34	194.28
E_{DHW}	74.16	74.78	74.41	74.15
$E_{SST,consumed}$	250.09	250.85	252.16	250.73
$E_{SST,feed-in}$	315.84	316.22	295.14	328.53
$E_{loss,SL}$	89.70	89.81	92.58	85.04
$E_{feed,pump}$	1.05	1.59	0.63	0.73

Table 3: Energy Ratios (unit: %)

Case	Base	ΔP+1bar	T_s+10°C	T_r-10°C
$\eta_{solar,field}$	47.5	47.5	45.1	49.0
$\eta_{solar,plant}$	43.8	43.8	40.9	45.4
$\eta_{self\_vs\_cons}$	6.3	6.1	5.7	6.2
$\eta_{self\_vs\_solar}$	5.1	5.0	5.0	4.8
$\eta_{pump\_vs\_solar}$	0.32	0.48	0.20	0.21

5. CONCLUSIONS

The present paper presented the modelling of a specific architecture of two-way substation together with the solar field and the consumer connected to it. Real DHN operating conditions were used as boundary conditions to dynamically simulate two days of operation. The latter showed that the developed framework was appropriate to perform detailed thermo-hydraulic simulations of such solar two-way substations.

Further steps will include the generalization of these results on seasonal and yearly basis, the simulations of the other promising architectures and the evaluation of the influence of a storage.

ACKOWLEDGEMENTS

This project has received funding from the European Union's Horizon 2020 research and innovation program under grant agreement No 723562. The authors also wish to thank Bosch Thermotechnik GmbH and Giroa-Veolia for their valuable inputs.

REFERENCES

Beckenbauer, D., Ehrenwirth, M., Klärner, M., Zörner, W., Cheng, V., 2017. Validation of a District Heating System Model and Simulation-Based Investigation of Bidirectional Heat Transport by Decentralized Solar Thermal Plants. Presented at the SWC/SHC 2017, Abu Dhabi, UAE.

Brange, L., Englund, J., Lauenburg, P., 2016. Prosumers in district heating networks – A Swedish case study. Appl. Energy 164, 492–500. https://doi.org/10.1016/j.apenergy.2015.12.020

COSTIC, 2016. besoin-eau-chaude-sanitaire-habitat-individuel-et-collectif.pdf (Guide Technique : Les besoins d'eau chaude sanitaire en habitat individuel et collectif).

Giraud, L., Baviere, R., Vallée, M., Paulus, C., 2015. Presentation, Validation and Application of the DistrictHeating Modelica Library. pp. 79–88. https://doi.org/10.3384/ecp1511879

Hassine, I.B., Eicker, U., 2014. Control Aspects of Decentralized Solar Thermal Integration into District Heating Networks. Energy Procedia, Proceedings of the 2nd International Conference on Solar Heating and Cooling for Buildings and Industry (SHC 2013) 48, 1055–1064. https://doi.org/10.1016/j.egypro.2014.02.120

Heymann, M., Rühling, K., Felsmann, C., 2017. Integration of Solar Thermal Systems into District Heating – DH System Simulation. Energy Procedia, 15th International Symposium on District Heating and Cooling, DHC15-2016, 4-7 September 2016, Seoul, South Korea 116, 394–402. https://doi.org/10.1016/j.egypro.2017.05.086

IEA SHC, 2004. Recommendation: Converting solar thermal collector area into installed capacity (m2 to kWth).

Jordan, U., Vajen, K., 2005. DHWcalc: Program to generate domestic hot water profiles with statistical means for user defined conditions, in: ISES Solar World Congress. pp. 1–6.

Lamaison, N., Baviere, R., Cheze, D., Paulus, C., 2017. A multi-criteria analysis of bidirectional solar district heating substation architecture. Presented at the SWC/SHC 2017, Abu Dhabi, UAE.

Lennermo, G., Lauenburg, P., 2016. Distributed heat generation in a district heating system. Presented at the International Conference on Solar-Heating and Cooling, Gleisdorf, Austria.

Lund, H., Werner, S., Wiltshire, R., Svendsen, S., Thorsen, J.E., Hvelplund, F., Mathiesen, B.V., 2014. 4th Generation District Heating (4GDH). Energy 68, 1–11. https://doi.org/10.1016/j.energy.2014.02.089

Meteonorm, 2017. Meteonorm: Irradiation data for every place on Earth [WWW Document]. URL http://www.meteonorm.com/en/ (accessed 7.10.17).

NF EN ISO 9806, 2017.

Paulus, C., Papillon, P., 2014. Substations for Decentralized Solar District Heating: Design, Performance and Energy Cost. Energy Procedia 48, 1076–1085. https://doi.org/10.1016/j.egypro.2014.02.122

Perez, R., Ineichen, P., Seals, R., Michalsky, J., Stewart, R., 1990. Modeling daylight availability and irradiance components from direct and global irradiance. Sol. Energy 44, 271–289. https://doi.org/10.1016/0038-092X(90)90055-H

Rosemann, T., Heymann, M., Rühling, K., Hafner, B., 2017a. DH Networks - Concept, Construction and Measurements Results of a Decentralized Feed-In Substation. Presented at the SWC/SHC 2017, Abu Dhabi, UAE.

Rosemann, T., Löser, J., Rühling, K., 2017b. A New DH Control Algorithm for a Combined Supply and Feed-In Substation and Testing Through Hardware-In-The-Loop. Energy Procedia, 15th International Symposium on District Heating and Cooling, DHC15-2016, 4-7 September 2016, Seoul, South Korea 116, 416–425. https://doi.org/10.1016/j.egypro.2017.05.089

SavoSolar SF500-15DG - Solar Keymark, 2016.

Schäfer, K., Schmidt, T., 2016. Technical challenges for solar thermal plants with decentralized feed-in into district heating networks and deduced plant concept for the experimental feed-in station in the SWD.SOL project. Presented at the 4th International Solar District Heating Conference, Billund, p. 8.

Schweiger, G., Larsson, P.-O., Magnusson, F., Lauenburg, P., Velut, S., 2017. District heating and cooling systems – Framework for Modelica-based simulation and dynamic optimization. Energy. https://doi.org/10.1016/j.energy.2017.05.115

Solar Keymark Database [WWW Document], 2018. URL http://www.solarkeymark.dk/CollectorCertificates (accessed 3.22.18).

Wetter, M., Fuchs, M., Grozman, P., Helsen, L., Jorissen, F., Lauster, M., Dirk, M., Nytsch-geusen, C., Picard, D., Sahlin, P., Thorade, M., 2015. IEA EBC Annex 60 Modelica library an international collaboration to develop a free open-source model library for buildings and community energy systems. Presented at the BS2015, pp. 395–402.

Wetter, M., Zuo, W., Nouidui, T.S., 2011. Modeling of heat transfer in rooms in the Modelica" Buildings" library. Lawrence Berkeley National Lab.(LBNL), Berkeley, CA (United States).

Wetter, M., Zuo, W., Nouidui, T.S., Pang, X., 2014. Modelica Buildings Library. J. Build. Perform. Simul. 7, 253–270.